Resonance Raman, Optical Spectroscopic, and EPR Characterization of the Higher Oxidation States of the Water Oxidation Catalyst, *cis,cis*-$[(bpy)_2Ru(OH_2)]_2O^{4+}$

Hiroshi Yamada[†] and James K. Hurst*[,‡]

Contribution from the Departments of Chemistry, National Defense Academy, 1-10-20 Hashirimizu, Yokosuka, Kanagawa 239, Japan, and Washington State University, Pullman, Washington 99164-4630

Received November 4, 1999

Abstract: Resonance Raman (RR) and optical spectroelectrochemical titrations of the *cis,cis*-$[(bpy)_2Ru(OH_2)]_2O^{4+}$ ion (denoted [3,3] to indicate the formal oxidation state of the Ru−O−Ru unit) were made over the range 0.8−2.0 V vs Ag/AgCl in 0.5 M trifluoromethanesulfonic acid; the results revealed sequential accumulation of three higher oxidation states. Two of these states were identified by redox titration with $Os(bpy)_3^{2+}$ as one-electron ([3,4]) and four-electron oxidized species ([5,5]); spectroscopic analysis of reaction products formed upon mixing the [3,3] and [5,5] ions indicated that the third oxidation state is a two-electron oxidized species ([4,4]). The [5,5] ion underwent first-order decay to the [4,4] ion with a rate constant, $k \simeq 9.5 \times 10^{-3}$ s^{-1}, that was nearly identical with the catalytic turnover rate for O_2 evolution, $k_{cat} \simeq 1.3 \times 10^{-2}$ s^{-1} measured under comparable conditions. The [4,4] ion underwent degradation more slowly to the [3,4] ion, which was stable on these time scales. An analogue bearing 4,4′-dimethyl-2,2′-bipyridine ligands exhibited very similar behavior, except that the oxidation steps were shifted by ∼50 mV to lower potentials. ^{18}O isotope labeling experiments on the underivatized complex established that there was no oxygen exchange at the bridging μ-oxo position during catalytic turnover. Frozen solutions of the [5,5] ion displayed unusual low-temperature spectroscopic features, including the following: (i) a narrow $g = 2.02$ axial EPR signal exhibiting an apparent six-line hyperfine interaction from a minor component; (ii) a concentration-dependent broad rhombic EPR signal in mixtures also containing the [4,4] ion; and (iii) a concentration-dependent replacement of its characteristic ruthenyl Ru═O stretching mode at 818 cm^{-1} in the RR spectrum when chemically oxidized with Ce^{4+} by an ^{18}O isotope sensitive set of three bands in the 650 cm^{-1} region. The RR spectrum of this new species is consistent with further coordination of the terminal oxo ligands by Ce^{4+} to form additional ligand bridges.

Introduction

Studies of mechanisms of water oxidation catalyzed by transition metal complex ions are inherently interesting because they present well-defined systems for investigating the complex multistep noncomplementary reactions associated with dioxygen O−O bond formation. In addition to defining minimum requirements for these chemical processes, these studies can be expected to provide insight into O−O bond-cleaving and bond-forming reactions occurring within metalloproteins[1−4] and the tetranuclear Mn cluster comprising the photosystem II oxygen-evolving complex,[4−7] and may be of importance to the design of practical devices for large-scale energy utilization.[8] Certainly, the most intensively studied of the reported homogeneous water oxidation catalysts have been ruthenium μ-oxo dimeric ions with the general formula *cis,cis*-$[L_2Ru(OH_2)]_2O^{n+}$, where L is 2,2′-bipyridine, a functionalized congener, or related diimines.[9] However, despite the attention given to these reactions, fundamental mechanistic issues such as the identities of detectable oxidation states and rate-limiting steps in the overall catalytic cycles, the identity and structure of the O_2-evolving species, and the identity of the immediate reaction product, e.g., H_2O_2 or O_2, are still unresolved. In this paper, we present evidence obtained from a variety of experimental techniques that resolves the first of these issues. A key feature of these studies has been the ability to electrochemically prepare highly oxidized samples of the catalyst for physical characterization using a columnar-flow carbon fiber electrode. Our results and conclusions differ considerably from recent publications on reactions of this catalyst that have relied extensively upon global kinetic analysis of spectrophotometrically detected reaction transients.[10]

* Address correspondence to this author. E-mail: hurst@wsu.edu. Fax: (509) 335-7848.

[†] National Defense Academy.

[‡] Washington State University.

(1) Iwata, S.; Ostermeier, C.; Ludwig, B.; Michel, H. *Nature* **1995**, *376*, 660−669. Tsukihara, T.; Aoyama, H.; Yamashita, E.; Tomizaki, T.; Yamaguchi, H.; Shinzawa-Itoh, K.; Nakashima, R.; Yaono, R.; Yoshikawa, S. *Science* **1995**, *269*, 1069−1074.

(2) Ortiz de Montellano, P. R. *Cytochrome P-450: Structure, Mechanism, and Biochemistry*; Plenum Press: New York, 1986.

(3) Feig, A. L.; Lippard, S. J. *Chem. Rev.* **1994**, *94*, 759−805.

(4) Wieghardt, K. *Angew. Chem., Int. Ed. Engl.* **1989**, *28*, 1153−1172.

(5) *Manganese Redox Enzymes*; Pecoraro, V. L., Ed.; VCH: New York, 1992.

(6) Yachandra, V. K.; Sauer, K.; Klein, M. P. *Chem Rev.* **1996**, *96*, 2927−2950.

(7) Dole, F.; Diner, B. A.; Hoganson, C. W.; Babcock, G. T.; Britt, R. D. *Acc. Chem. Res.* **1998**, *31*, 18−25. Tommos, C.; Mccracken, J.; Styring, S.; Babcock, G. T. J. *Am. Chem. Soc.* **1998**, *120*, 10441−10452.

(8) *Energy Resources through Photochemistry and Catalysis*; Grätzel, M., Ed.; Academic Press: New York, 1983. *Photochemical Conversion and Storage of Solar Energy*; Connolly, J. S., Ed; Academic Press: New York, 1981.

(9) Extensive compilations of earlier papers are given in refs 10 and 15.

10.1021/ja993914y CCC: $19.00
Published on Web 05/18/2000

Experimental Section

Materials. The μ-oxo-bridged dimeric ruthenium coordination complexes were prepared from monomeric *cis*-$L_2Ru^{II}Cl_2$ precursors using well-established synthetic procedures.[11] Briefly, these procedures involved heating aqueous solutions of the precursor in the presence of 2 equiv of $AgNO_3$, filtration of the accumulated AgCl, overnight crystallization following addition of a suitable precipitant, and subsequent recrystallization from aqueous solutions until reproducible optical properties were obtained. For these preparations, repeated recrystallization of the initial products was required to remove relatively insoluble minor impurities that had visible bands that strongly overlapped those of the "blue" dimers, i.e., the complexes in their [3,3] oxidation states. Although these impurities were difficult to detect in the spectra of the [3,3] ions, they could be easily identified by oxidative titration of solutions of the product salts with Ce^{4+}. Specifically, addition of substoichiometric amounts of Ce^{4+} caused preferential oxidation of the [3,3] product ion to its "orange" [3,4] state, characterized by a visible band at ~450 nm; the residual unoxidized impurity exhibited a symmetric band centered at ~650 nm, which was distinguishable from the product [3,3] ion primarily by the absence of a high energy shoulder on its visible band. The impurity could be oxidized upon further addition of Ce^{4+} to give a relatively weakly absorbing species with a visible band at ~550 nm. Thus, the presence of even very small amounts of the impurity caused loss of isosbestic points in [3,3] → [3,4] spectral titrations. The *cis*,*cis*-$[(bpy)_2Ru(OH_2)]_2O^{4+}$ ion obtained by this procedure was isolated as the perchlorate salt and gave $\epsilon_{636} = 2.2 \times 10^4$ M^{-1} cm^{-1} in 0.5 M CF_3SO_3H, compared to a literature value of $\epsilon_{636} = 2.1 \times 10^4$ M^{-1} cm^{-1}.[11] (CAUTION: perchlorate salts of these ions are potentially explosive. Meyer and co-workers report that a precipitate of highly oxidized μ-oxo dimer isolated from perchlorate solutions ignited during preparation for IR analyses (T. J. Meyer, personal communication).) The *cis*,*cis*-$[(DMB)_2Ru(OH_2)]_2O^{4+}$ analogue (DMB = 4,4′-dimethyl-2,2′-bipyridine) was isolated as the hexafluorophosphate salt; extinction coefficients for this and the one-electron oxidized *cis*,*cis*-$[(DMB)_2Ru(OH_2)]_2O^{5+}$ ion were determined by titration with standard Ce^{4+} ion to be $\epsilon_{640} = 2.0 \times 10^4$ M^{-1} cm^{-1} and $\epsilon_{452} = 2.5 \times 10^4$ M^{-1} cm^{-1}, respectively, in 1 M CF_3SO_3H. The *cis*-$(DMB)_2Ru^{II}Cl_2$ precursor was prepared by refluxing ruthenium trichloride with 2 equiv of DMB in dimethylformamide that contained hydroquinone and LiCl. Upon cooling, the volume was increased 2.5-fold by adding water and the solution stored overnight in a refrigerator. The crystalline product was recovered by filtration and washed with water. Tris(2,2′-bipyridine)-osmium(II) perchlorate was prepared by refluxing $(NH_4)OsCl_6$ with 3 equiv of 2,2′-bipyridine,[12] followed by reduction of the volume and addition of an aqueous saturated $NaClO_4$ solution. The crystals obtained upon cooling were redissolved in hot water, filtered to remove insoluble material, and recrystallized by addition of $NaClO_4$. Triflic acid (CF_3SO_3H) was redistilled under vacuum and stored at 4 °C as a 1 M aqueous solution. Other chemicals were reagent grade and used as received from commercial suppliers; water was purified using a Milli-Q ion exchange/reverse osmosis system.

Analytical Methods. Potentiometric titration of the *cis*,*cis*-$[L_2Ru(OH_2)]_2O^{4+}$ ions (hereinafter, denoted as [3,3])[13] was accomplished using a columnar carbon fiber electrolysis flow cell (Model HX-201, Hokuto Denko (Tokyo)) that contained an electrode surface area of ~3000 cm^2 in a working volume of 2 mL. Acidic solutions of the [3,3] ion were pumped through the cell at flow rates of 1−2 mL/min using either a Buchler multistaltic pump or, where more precise flows were desired, a Harvard Instruments PHD 2000 syringe pump. The redox potential of the cell, referenced against a Ag/AgCl electrode, was controlled using an EG&G/PAR Model 273 potentiostat/galvanostat. The general procedure followed for these experiments was to pass triflic acid solutions through the electrolysis cell at the highest potential to be used (usually 1.54 V) until the anodic current dropped to a steady value, following which the [3,3]-containing solution was introduced at the desired potential. Without preconditioning the cell in this manner, which apparently oxidizes functional groups on the carbon fibers, it was difficult to reproducibly obtain completely oxidized samples at the highest potentials used in the potentiometric titrations. Adsorption of the oxidized dimers to the carbon electrode was also evident from the observation that the first few milliliters of effluent contained significantly lower concentrations of the dimer than was introduced. However, once adsorption sites were saturated, the system reproducibility was excellent, with relative amounts of the various oxidized species in effluent solutions changing rapidly and reversibly to increases and decreases in the applied cell potential. Upon completion of an experiment, the cell potential was adjusted to 0.4 V and the triflic acid solution was again passed through the cell until the effluent was colorless; the electrode was then washed with H_2O. This procedure removed the adsorbed ruthenium complexes. Treated in this manner, the flow electrolysis system gave reproducible results over a period of months on numerous different sample preparations.

Resonance Raman spectra of the electrochemically oxidized complexes were measured in glass capillaries that were directly connected to the cell by Teflon tubing. The most highly oxidized samples underwent slow photodecomposition when exposed to the laser beam; this interference was eliminated by slowly flowing the samples through the illuminated region. Photodecomposition did not interfere with low-temperature measurements of chemically oxidized complexes; in these studies, samples were oxidized to a desired level with Ce^{4+} ion, and portions were rapidly transferred to capillary tubes and stored in liquid N_2, then transferred to a low-temperature optical Dewar flask[15] maintained at ~90 K for analysis. Raman spectra were obtained by using a McPherson 2061 spectrograph and Princeton Instruments LN-1100PB CCD detector;[16] excitation sources were Coherent Innovia 90-6 Ar and Innovia 302 Kr lasers. For solutions, spectra were acquired using 90° scattered light; for Ce^{4+}-oxidized frozen samples, spectra were acquired from backscattered light. Peak frequencies were calibrated by using an indene standard, and are accurate to ±1 cm^{-1}.

Optical spectra of the electrochemically oxidized ions were obtained using a Hewlett-Packard 8452A diode array spectrophotometer either by mounting a glass capillary connected to the electrolysis cell in the sample chamber or, where quantitative measurement of apparent ϵ-values was desired, by transferring effluent solution manually into optical cuvettes. The oxidizing equivalents were determined by reacting effluent solutions at various times following electrolysis with a 5-fold molar excess of $Os(bpy)_3^{2+}$; the extent of reaction was determined by using an $Os(bpy)_3^{2+} - Os(bpy)_3^{3+}$ difference extinction coefficient of $\Delta\epsilon_{480} = 1.38 \times 10^4$ M^{-1} cm^{-1}.[17] The reaction stoichiometry was confirmed by titrating 0.12 mM solutions of electrochemically prepared [3,4] ion with $Os(bpy)_3^{2+}$; complete reduction to the [3,3] ion (measured at 638 nm) occurred when the reactant solutions contained a 1/1 $Os(bpy)_3^{2+}$/[3,4] molar equivalence.

Low-temperature electron paramagnetic resonance spectra were taken using a Brucker ESP 300E X-band instrument equipped with an APD Cryogenics Heli-Tran liquid He cryostat; effluent samples from the electrochemical cell were manually loaded into EPR tubes and immediately immersed in liquid N_2 for subsequent analysis.

(10) Chronister, C. W.; Binstead, R. A.; Ni, J.; Meyer, T. J. *Inorg. Chem.* **1997**, *36*, 3814−3815.

(11) Gilbert, J. W.; Eggleston, D. S.; Murphy, W. A., Jr.; Geselowitz, D. A.; Gersten, S. W.; Hodgson, D. J.; Meyer, T. J. *J. Am. Chem. Soc.* **1985**, *107*, 3855−3864.

(12) Johnson, S. R.; Westmoreland, T. D.; Caspar, J. V.; Barqawi, K. R.; Meyer, T. J. *Inorg. Chem.* **1988**, *27*, 3195−3200.

(13) This notation is intended to imply the net oxidation level of the μ-oxo ions only. The Ru−O−Ru unit is best described as a three-center bond, over which the metal and bridging oxygen electrons are extensively delocalized.[14] Thus, [3,4] indicates that there are 13 π-symmetry and nonbonding electrons in the unit (including 4 from O^{2-}), not that there exist discrete charge-localized ruthenium d^5 and d^4 centers in the ion. Similarly, [3,3] indicates that there are 14 π and nonbonding electrons in the unit, etc.

(14) Weaver, T. R.; Meyer, T. J.; Adeyemi, S. A.; Brown, G. M.; Eckberg, R. P.; Hatfield, W. E.; Johnson, E. C.; Murray, R. W.; Untereker, D. *J. Am. Chem. Soc.* **1975**, *97*, 3039−3048.

(15) Lei, Y.; Hurst, J. K. *Inorg. Chem.* **1994**, *33*, 4460−4467.

(16) Nakamura, N.; Moënne-Loccoz, P.; Tanizawa, K.; Mure, M.; Suzuki, S.; Klinman, J. P.; Sanders-Loehr, J. *Biochemistry* **1997**, *36*, 11479−11486.

(17) Szentrimay, R.; Yeh, P.; Kuwana, T. *ACS Symp. Ser.* **1977**, *38*, 143−169.

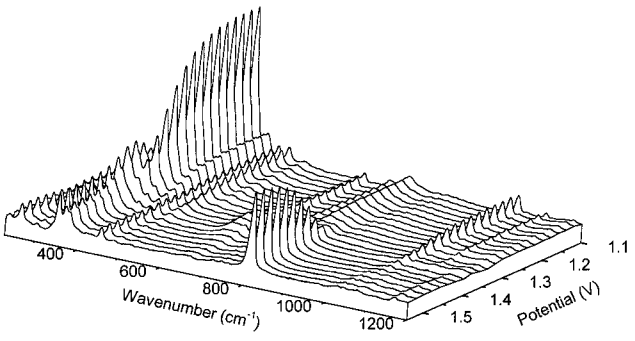

Figure 1. Resonance Raman spectroelectrochemical titration of the μ-oxo dimer. Solutions of 0.25 mM [3,3] ion in 0.5 M triflic acid were passed at ~1 mL/min through the electrochemical flow cell at the potentials indicated and the RR spectrum was recorded at a point immediately following efflux from the cell using 488 nm excitation (25 mW, average of ten 3 s accumulations). Scattering intensities have been normalized to the intense 1040 cm^{-1} band of CF_3SO_3H; all bands from triflic acid have been computer-subtracted from the displayed spectra.

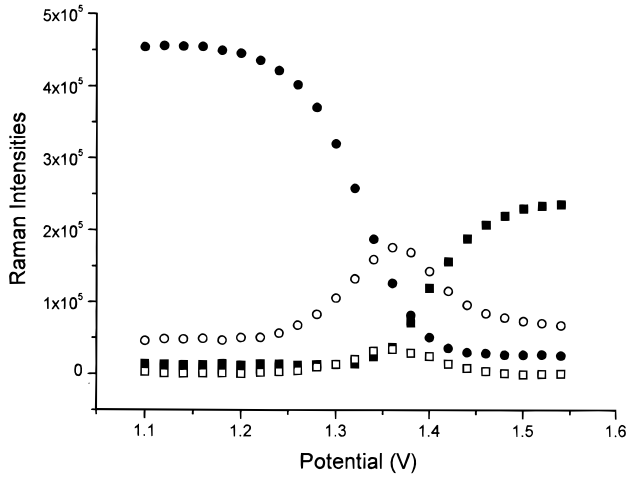

Figure 2. Relative intensities of selected RR bands at various potentials: 358 (○), 389 (●), 640 (□), and 818 cm^{-1} (■). Data are from Figure 1.

Results and Discussion

Resonance Raman Spectra at Various Redox Poises. When solutions of the μ-oxo ions were passed through a carbon fiber electrolysis cell, their resonance Raman (RR) spectra changed in a manner indicative of progressive oxidation with increasing applied potential. A typical result is given in Figure 1 for a 250 μM solution of the [3,3] ion in 0.5 M triflic acid under 488 nm excitation. Three species are evident from the redox electrochemical titration. These include the [3,4] ion,[13] which was formed from the [3,3] ion at potentials above ~0.8 V under these conditions.[11] The [3,4] ion was replaced by an intermediary species at ~1.3 V, which is characterized by a moderately strong vibration at 358 cm^{-1} and weaker broad band centered at ~640 cm^{-1}. This intermediate, in turn, gave way at ~1.4 V to the most highly oxidized species, which is characterized by a strong band at 818 cm^{-1} and several weaker bands in the 350 cm^{-1} region. The titrimetric behavior of these systems is clearly revealed in plots of the normalized relative intensities of these bands vs applied potential (Figure 2). Analogous behavior was observed for the *cis,cis*-$[(DMB)_2Ru(OH_2)]_2O^{4+}$ ion in 0.5 M triflic acid, except that the breakpoints in the titration curves for formation of the intermediary and highest oxidized species occurred at ~50 mV lower potentials, consistent with the more facile oxidation of Ru μ-oxo dimers bearing electron-donating ring substituents.[18]

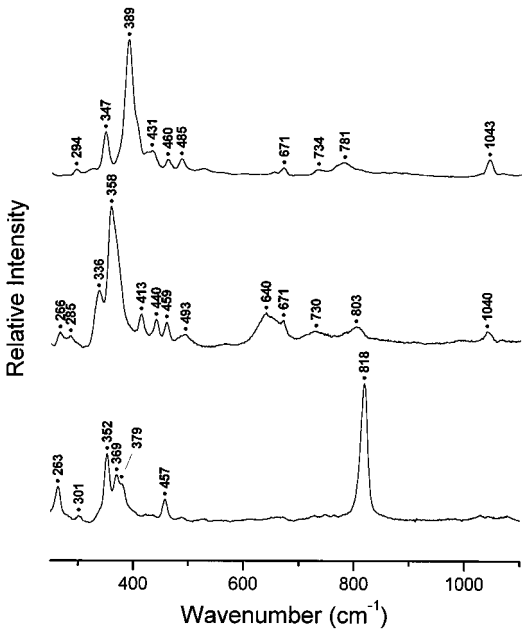

Figure 3. Resonance Raman spectra of the ruthenium dimer in various oxidation states. Upper trace, [3,4] ion; middle trace, [4,4] ion; lower trace, [5,5] ion. Data are from Figure 1, normalized to the most intense peak in the spectrum. The spectrum of the [4,4] ion was determined by subtracting contributions from the [3,4] and [5,5] ions at 1.36 V to the overall spectrum. The percentage amounts of these ions were calculated from the spectroelectrochemical titration data of Figure 2 to be 17% ([3,4]) and 7.9% ([5,5]) of the total dimer concentration.

The bands at 389, 358, and 369 cm^{-1} in the RR spectra (Figure 3) of the [3,4], intermediate, and highest oxidation states, respectively, can be assigned to the Ru−O−Ru symmetric stretching mode for these complexes based upon their position in the RR spectrum (350−400 cm^{-1})[19] and the small shifts to lower energies observed upon isotopic substitution of ^{18}O for ^{16}O in the bridging oxygen atom,[20] specifically, at 382, 356, and 364 cm^{-1} in the corresponding ^{18}O-derivatives. The magnitude of the induced shifts indicates that the Ru−O−Ru bridges are nearly linear.[15,21] The 818 cm^{-1} band in the most highly oxidized ion has been assigned to a ruthenyl (Ru═O) stretching mode, based upon the spectral characteristics in water containing varying $^{16}O/^{18}O$ ratios.[21] Consistent with this assignment, ^{18}O isotopic substitution into the cis-aqua positions followed by complete oxidation by addition of excess Ce^{4+} caused this peak to shift ~40 cm^{-1} to lower energies.

The RR spectra were insensitive to flow rates through the electrolysis cell in the range of 1−2 mL/min, and were basically unchanged upon increasing the acidity to 1 M. The intensity of the 818 cm^{-1} band was markedly suppressed at acidities below 0.1 M, however, and higher potentials were required for formation of the intermediary species under these conditions. Background currents arising from solvent oxidation to O_2 became appreciable above pH 1, so the probable cause of these effects is inability to attain redox equilibrium in the flow cell.

(18) Zhou, J., Ph.D. Dissertation, Oregon Graduate Institute of Science & Technology, 1990.
(19) Wing, R. M.; Callahan, K. P. *Inorg. Chem.* **1969**, *8*, 871−874.
(20) Sanders-Loehr, J.; Wheeler, W. D.; Shiemke, A. D.; Averill, B. A.; Loehr, T. M. *J. Am. Chem. Soc.* **1989**, *111*, 8084−8093.
(21) Hurst, J. K.; Zhou, J.; Lei, Y. *Inorg. Chem.* **1992**, *31*, 1010−1017.

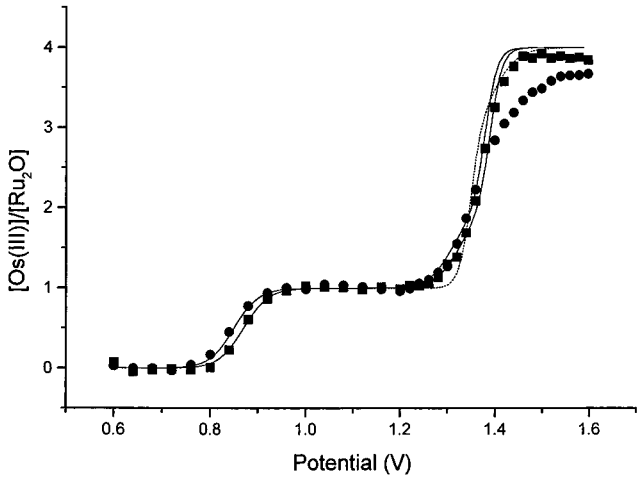

Figure 4. Oxidizing equivalents of flow-electrolyzed solutions of the μ-oxo dimer. For these measurements, 0.2 mL aliquots of 0.25 mM dimer in 0.5 M (■) or 0.1 M (●) triflic acid at various potentials were immediately quenched with 1 mL of 0.25 mM $Os(bpy)_3^{2+}$. The solid lines are the calculated fits assuming the intermediate is the [4,4] ion, with $E_1^o = 0.87$ (pH 0.3) or 0.85 V (pH 1.0), $E_2^o = 1.325$ (pH 0.3) or 1.31 V (pH 1.0), and $E_3^o = 1.39$ (pH 0.3) or 1.38 V (pH 1.0); the dashed line is the calculated fit at pH 0.3 assuming the intermediate is the [4,5] ion with $E_1^o = 0.87$ V, $E_2^o = 1.35$ V, and $E_3^o = 1.40$ V. All potentials are referenced against Ag/AgCl (+0.20 V vs NHE).

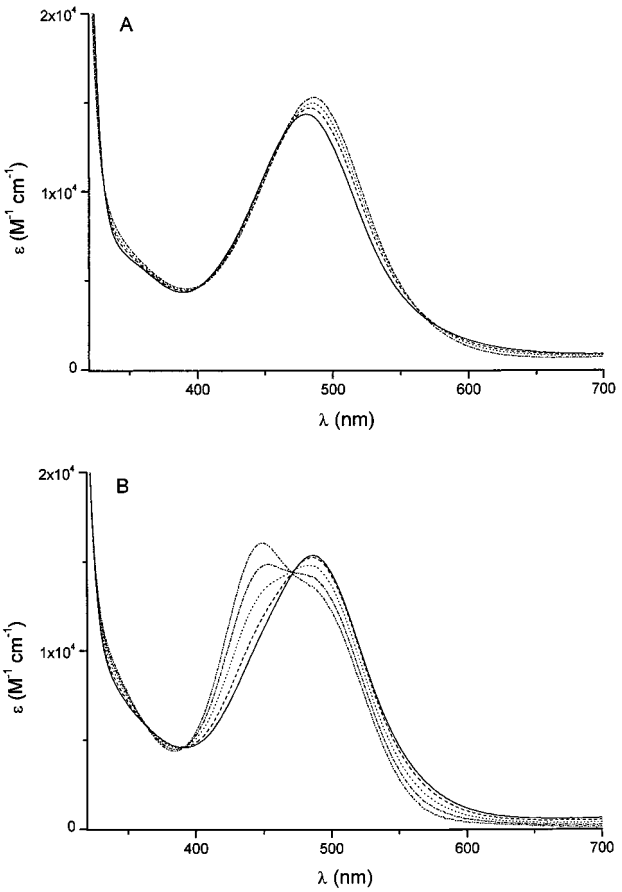

Figure 5. Optical changes following electrochemical oxidation of 0.25 mM μ-oxo dimer in 0.5 M triflic acid at 1.54 V. (Panel A) Conversion of the [5,5] ion to the intermediate: solid line, 30 s; dashed line, 90 s; dotted line, 150 s; dot−dashed line, 270 s. (Panel B) conversion of the intermediate to the [3,4] ion: solid line, 510 s; dashed line, 1050 s; dotted line, 2070 s; dot−dashed line, 2970 s; double dot−dashed line, 4770 s.

Oxidation State of the Most Highly Oxidized Species. The number of oxidizing equivalents in the effluent from the electrochemical flow cell was determined spectrophotometrically by measuring the amount of $Os(bpy)_3^{3+}$ formed upon reaction with excess $Os(bpy)_3^{2+}$ ion. This ion has a reduction potential ($E° = 0.60$ V vs Ag/AgCl)[17] that is appropriate for quantitative reduction of higher oxidation states to the [3,3] state without forming the more reduced species that undergo irreversible decomposition by cleavage of the μ-oxo bridge.[11] The extent of $Os(bpy)_3^{2+}$ oxidation is plotted as a function of cell potential in Figure 4. The data clearly establish that in 0.5 M triflic acid the highest oxidation state corresponds to four electrons removed from the [3,3] ion, i.e., to the [5,5] ion;[13] the difficulty in achieving this state at lower acidities, noted above in the RR electrochemical titration, is also apparent here from the maximal extent of oxidation ($[Os(bpy)_3^{3+}]/[Ru_2O] \simeq 3.6$) obtained at pH 1.

In principle, the shape of the $Os(bpy)_3^{3+}$ titration curve could be used to identify the oxidation state of the intermediary species observed in the RR spectra (Figures 1 and 2), which is either [4,4] or [4,5]. However, the uncertainty in relevant redox potentials is relatively large, so that reasonable fits could be obtained for either the sequence [3,3] → [3,4] → [4,4] → [5,5] (with $E_1^o = 0.87$ V, $E_2^o = 1.32$ V, and $E_3^o = 1.38$ V) or the sequence [3,3] → [3,4] →[4,5] → [5,5] (with $E_1^o = 0.87$ V, $E_2^o = 1.35$ V, and $E_3^o = 1.40$ V) (Figure 4). Furthermore, the two oxidation steps were only quasireversible at the carbon fiber electrode, precluding determination of the number of electrons transferred from the slopes of the corresponding Nernst plots. (For example, slopes of E vs log[ox]/[red] obtained from the data in Figure 2 were 73 mV for [3,4] ⇌ intermediate and 55 mV for intermediate ⇌ [5,5].) Nonetheless, it proved possible to unambiguously identify the oxidation state of the intermediate using the flow-kinetic methods described in the following paragraphs.

Visible Absorption Spectra. Optical spectra of the intermediate and [5,5] ions in 0.5 M triflic acid were determined by sampling the effluent from the electrolysis cell poised at various potentials. Below 1.1 V, the oxidized solution contained only the [3,4] ion, which gave an asymmetrical band exhibiting a maximum absorption at 450 nm and a pronounced low-energy shoulder at ∼490 nm (for example, the spectrum labeled as 4770 s in Figure 5B); the shoulder can be assigned to the species $[(bpy)_2(OH_2)Ru^{III}ORu^{IV}(OH)(bpy)_2]^{4+}$, formed at this pH by deprotonation of one of the aqua ligands ($pK_a = 0.4$).[11] With progressive increase in the applied potential over the range 1.25−1.4 V, the spectrum of the [3,4] ion gave way to a new symmetrical band at ∼490 nm, which decreased slightly in intensity and shifted to 482 nm at higher potentials. Above ∼1.45 V, no further changes were observed in the optical spectrum. Thus, the dependence of the optical spectra upon cell potentials paralleled the dependence observed for the RR spectra (Figure 1). From the redox titration with $Os(bpy)_3^{3+}$ (Figure 4), the 482 nm peak can be assigned to the [5,5] ion, for which $\epsilon_{482} = 1.5 \times 10^4\ M^{-1}cm^{-1}$. This spectrum is essentially identical with the one obtained by Lei and Hurst upon oxidizing the [3,3] ion with a large excess of Ce^{4+} in 1 M triflic acid.[15] The optical spectrum of the intermediate was measured in two ways: (i) by subtracting the contribution of the [3,4] ion from the spectrum obtained upon electrochemically oxidizing the solution to 1.32 V using the corresponding RR spectra (Figures 1 and 2) to determine the relative concentrations of the two species and (ii) by monitoring spectral changes accompanying progressive

decay of the [5,5] ion which, as described below, leads to nearly quantitative accumulation of the intermediate. Both methods gave equivalent results, indicating a symmetrical visible band for the intermediate centered at 488 nm, for which $\epsilon_{488} = 1.6 \times 10^4$ M^{-1} cm^{-1}. Visible absorption spectra for the intermediate and [5,5] oxidation states are indicated in Figure 5A as the spectra taken at 270 and 30 s, respectively.

Decay Kinetics of the Reactive Species. The [5,5] ion decayed relatively rapidly to the intermediate species, which then underwent relatively slow decomposition to the [3,4] ion, which is stable on these time scales. Optical changes accompanying these transformations in 0.5 M triflic acid at room temperature are shown in Figure 5. The kinetics of decay of the [5,5] ion could be monitored by measuring the loss in intensity of the 818 cm^{-1} RR band (Figure 3) or absorbance changes accompanying the first step in the biphasic decay to the [3,4] ion (Figure 5A). In either case, the data fitted a first-order rate law, for which $t_{1/2} = 74 \pm 8$ s ($k = 9.5 \times 10^{-3}$ s^{-1}) under these conditions. The rate constant was independent of the initial [5,5] ion concentration over the range examined (0.12−0.50 mM), but increased with decreasing triflic acid concentration, i.e., $k = 6 \times 10^{-3}$ s^{-1} in 1.0 M triflic acid and 2×10^{-2} s^{-1} in 0.1 M triflic acid. Somewhat surprisingly, the [5,5] ion of the DMB analogue gave an identical decomposition rate constant, $k = 9.9 \times 10^{-3}$ s^{-1}, in 0.5 M triflic acid.

The kinetics of conversion of the intermediate to the [3,4] ion has not been examined in detail, but is clearly temporally well-resolved from the decay of the [5,5] ion to the intermediate (Figure 5B). This same general reaction behavior was observed when the [3,3] ion was reacted with chemical oxidants. For example, addition of a 15-fold excess of Ce^{4+} ion to 0.2 mM [3,3] in 0.5 M triflic acid gave immediate formation of the [5,5] ion, which could be identified either by its characteristic 482 nm optical band (Figure 5) or 818 cm^{-1} RR band (Figure 3); after a few minutes, decomposition to the intermediate species was evident in either spectrum, which was followed by much slower conversion to the [3,4] ion. Thus, the reaction dynamics illustrated in Figure 5 are not peculiar to the method of generation of the [5,5] ion.

Oxidation State of the Intermediate. The ability to prepare, at least for short times, pure solutions of the [5,5] ion that contain no additional oxidant enables us to determine the oxidation state of the intermediate by a very simple experiment. Stoichiometric constraints require that only a single product will form upon flow-mixing equal amounts of electrochemically generated [5,5] ion with [3,3] ion if the intermediate is the [4,4] ion, i.e., [3,3] + [5,5] → 2[4,4], but that equal amounts of the [3,4] ion and intermediate will form if the intermediate is the [4,5] ion, i.e., [3,3] + [5,5] → [3,4] + [4,5]. A typical result of this experiment is shown in Figure 6. The immediate product solution exhibited a single optical band in the visible region with a maximum at 488 nm, clearly indicating that only the intermediate species was formed. Slow subsequent decomposition to the [3,4] ion was also observed, as expected. These results can only be interpreted as indicating that the intermediate is the [4,4] ion.[13]

A further test of this assignment can be made by determining the rate of loss of oxidizing equivalents in electrochemically prepared solutions of the [5,5] ion. If the [4,4] ion is the accumulating intermediate, then decay of the [5,5] ion should be accompanied by loss of one-half of the original oxidizing equivalents. In 0.5 M triflic acid, the [Os^{III}]/[Ru_2O] ratio decreased with time in a biphasic manner from an initial value of ∼3.9 (Figure 4) to ∼2 after 10 min, and then more slowly over a period of 1−2 h approached a limiting value of 1. Thus,

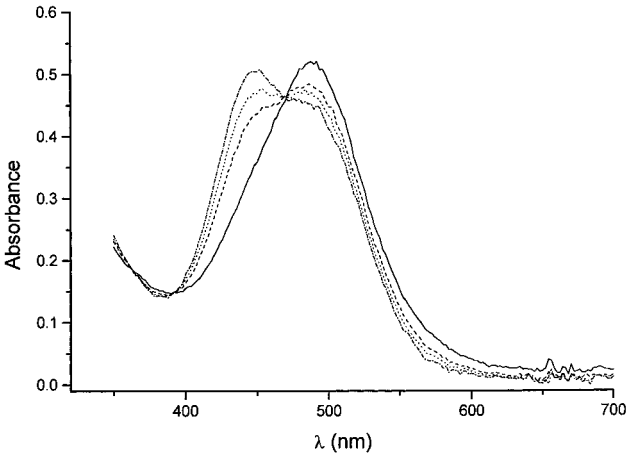

Figure 6. Optical spectral identification of [3,3] + [5,5] reaction products. A 0.5 M triflic acid solution containing 0.25 mM of the [3,3] ion was flow-mixed through a 12-jet tangential mixer with an equal amount of the [5,5] ion prepared by flow electrolysis at 1.54 V and the optical spectra recorded in a glass capillary mounted in a 2 mm spectral cell. Spectra shown were obtained immediately after stopping the flow (solid line) and after an additional 30 (dashed line), 60 (dotted line), and 120 min (dash−dotted line).

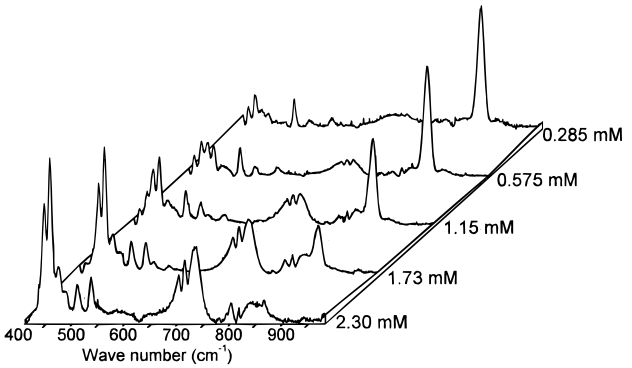

Figure 7. Concentration dependence of the low-temperature RR spectra of the [5,5] ion. Conditions: [3,3] ion at the indicated concentrations in 0.5 M triflic acid oxidized with 10-fold excess Ce^{4+} and immediately frozen at ∼90 K. RR spectra: 40 mW excitation at 488 nm, average of thirty 30 s accumulations.

rates of change in the oxidizing capabilities of electrochemically prepared solutions of the dimer paralleled rates of changes in the optical and RR spectra of complex ion, strongly supporting the assignment of a [5,5] → [4,4] → [3,4] decay sequence. A typical result is given as Figure S1 in Supporting Information.

Ce^{4+} Binding to the [5,5] Ion. In earlier studies, we had found that frozen solutions of the dimer oxidized with Ce^{4+} occasionally gave several new moderately intense RR bands in the 650−700 cm^{-1} region, but were unable to determine their origin.[15,21] As shown in Figure 7, this is a concentration-dependent phenomenon, with new bands appearing at 396, 407, 486, 652, 664, and 683 cm^{-1} at the expense of the 818 cm^{-1} band. The relative intensities of the major new bands were constant in the various RR spectra; furthermore, loss of intensity at 818 cm^{-1} was proportional to the increase at 407 cm^{-1}. These observations suggest that the new spectrum corresponds to a single species formed directly from the [5,5] monomer. However, the apparent concentrations calculated from the RR spectra do not fit simple monomer ⇌ multimer equilibrium models. In the experiment depicted in Figure 7, the Ce^{4+}/dimer ratio was kept constant at 10/1, so that both dimer and Ce^{4+} concentrations were changing. Thus, it is possible that the spectroscopic

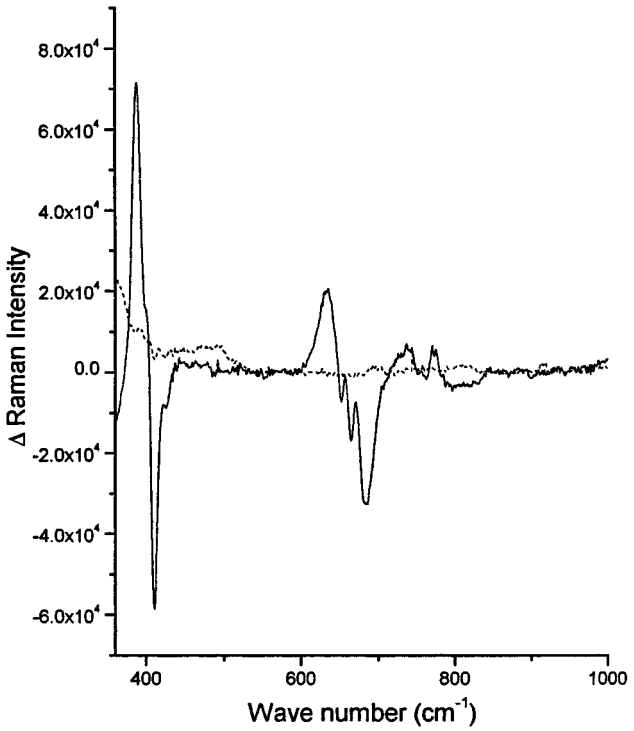

Figure 8. Resonance Raman difference spectra for the Ce^{4+}-associated [5,5] ion in 0.5 M triflic acid. Spectra were obtained by subtracting (a) the 90 K RR spectrum of 3.1 mM normal isotopic Ce^{4+}-oxidized [3,3] ion in $H_2{}^{16}O$ from the spectrum of 4.7 mM Ce^{4+}-oxidized ^{18}O-substituted [3,3] ion in 96% ^{18}O-H_2O (solid line) and (b) the spectrum of 3.2 mM Ce^{4+}-oxidized normal isotopic [3,3] ion in 99% D_2O from the corresponding spectrum in normal H_2O (dashed line). Spectra were taken with 40 mW RR excitation at 488 nm, average of ten 30 s accumulations. Scattering intensities have been normalized to the 1040 cm^{-1} band of CF_3SO_3H; all bands from triflic acid have been computer-subtracted from the displayed spectra.

changes are due to ion association between Ce^{4+} and the dimer. This was confirmed in a separate experiment in which the RR specta of 0.15 mM dimer mixed with 1.5 mM Ce^{4+} and with 15 mM Ce^{4+} were compared. The RR spectrum obtained at low Ce^{4+} matched that of the low concentration limit in Figure 7, whereas the spectrum at high Ce^{4+} matched that of the high concentration limit. From the data in Figure 7, one calculates an apparent Ce^{4+}−dimer 1/1 association constant of $K \approx 100$ M^{-1}.[22] In contrast to this low-temperature behavior, the RR spectra for the [5,5] ion at ambient temperatures gave no evidence of ion association, and were identical at all concentrations examined over the range 0.1−2.3 mM.

^{18}O isotopic substitution in the bridging oxo and coordinated aqua ligand positions of the Ce^{4+}-associated [5,5] ions caused the Ru−O−Ru symmetric stretching mode and new bands attributed to ion association to shift to lower energies. A difference spectrum displaying these shifts is given in Figure 8. The only other identifiable feature of the difference spectrum is a weak broad peak and trough structure at 780−820 cm^{-1} that can be assigned to the first overtone of the Ru−O−Ru stretching vibration.[21] No spectral shifts were observed when the normal isotopic Ce^{4+}-associated [5,5] ion was formed in D_2O (Figure 8, dashed line), suggesting that the normal coordinate vibrations giving rise to the 650−680 cm^{-1} bands do not involve solvent molecules or protonated oxo bridges. Prior work had established that the Ru−O−Ru bridging oxygen does not exchange with solvent H_2O in any of the dimer oxidation states, even during catalytic turnover.[21] These observations were confirmed in the present study by adding a 40-fold excess of Ce^{4+} to a 0.5 M triflic acid solution of water of normal isotopic composition containing 0.18 mM of the ^{18}O-substituted [3,4] ion. After ∼12 h at room temperature, the catalyst had cycled 10 times and the Ce^{4+} was completely reduced. At this point, the RR spectrum of the [3,4] ion was retaken and found to be identical with the spectrum before reaction. In particular, there was no shift in the shape or position of the Ru−O−Ru symmetric stretch at 382 cm^{-1}, which would have diminished in intensity with concomitant appearance of a 389 cm^{-1} band had any exchange occurred. In marked contrast to the substitution-inert character of the bridging O atom, water exchange with the cis-aqua ligands is rapid in the [3,3] oxidation state.[21,23] Thus, the ^{18}O isotope-sensitive bands in the 650 cm^{-1} region of the low-temperature spectra of the [5,5] ion (which were prepared by Ce^{4+} oxidation of the [3,3] ion in water of normal isotopic composition or 96% $H_2{}^{18}O$) can be assigned to motions of the cis-oxo ligands and, consequently, the RR spectroscopic changes in Figure 7 to Ce^{4+}-induced structural changes at these positions.

Electron Paramagnetic Resonance Spectra. Earlier low-temperature EPR studies on Ce^{4+}-oxidized complexes had revealed a broad pH-dependent rhombic signal at $g = 1.77-1.90$ for the [3,4] ion, which was sharply attenuated in strongly acidic media, and two additional signals in highly oxidized solutions comprising a broad signal whose major peak was at $g = 1.87$ and a relatively narrow, more isotropic signal centered at $g \approx 2$.[15] In part because large excesses of Ce^{4+} were required to reach the higher oxidation states, the relative signal intensities could not be reproducibly generated in redox titrimetric assays, and consequently assignment of the signals to particular species was provisional. By allowing precise regulation of the redox poise, the electrochemical flow method overcomes this deficiency. The general features previously observed in Ce^{4+}-oxidized samples are reproduced in electrochemically oxidized 1 mM samples of the μ-oxo dimer in 0.5 M triflic acid (Figure 9A). At 1.1 V, only the [3,4] ion was present in solution (Figures 1,2) and gave a broad rhombic signal with apparent g_x, g_y, and g_z values of 2.04, 1.79, and 1.72. Upon oxidation to the intermediary state at 1.3 V, the signal the band shape became more isotropic with loss of the g_x component and apparent $g_\perp$ and $g_\parallel$ values of 1.79 and 1.72. This band diminished in intensity with increasing potential and disappeared completely above 1.45 V, but was replaced by a narrower signal at $g = 2.02$ whose intensity was unchanged at potentials ≳1.4 V (Figure 9B). This latter signal was a prominent feature of all the highly oxidized samples whose concentrations ranged from 0.25 to 3.0 mM, and thus appears to be an intrinsic property of the [5,5] ion. The clean spectrum obtained reveals two previously unrecognized features of the signal, a second band component at $g = 1.90$ indicating axial magnetic symmetry and the appearance of satellite bands on the $g_\perp$ component, suggesting the existence

(22) The oxidation state(s) of the dimer in the Ce^{4+}-associated species is (are) unknown. This follows because oxidation with excess Ce^{4+} at room temperature initiates the catalytic cycle; upon subsequent freezing, Ce^{4+} could stabilize any of the accessible dimer oxidation states, causing it to accumulate. At present, only the [3,3] ion can be excluded; because this oxidation state is not resonance-enhanced under 488 nm excitation, it would not give a RR spectrum (Figure 7).

(23) Solvent exchange in the cis-aqua position of the [3,3] ion was measured by incubating an ^{18}O-substituted sample in normal isotopic H_2O, or vice-versa, then periodically oxidizing portions to the [5,5] state and determining the relative intensities of the ruthenyl Ru═O RR stretching bands at 818 (Ru═^{16}O) and 776 cm^{-1} (Ru═^{18}O). Under our experimental conditions, water exchange in the [3,3] ion was complete within 2 min (H. Yamada, unpublished observations).

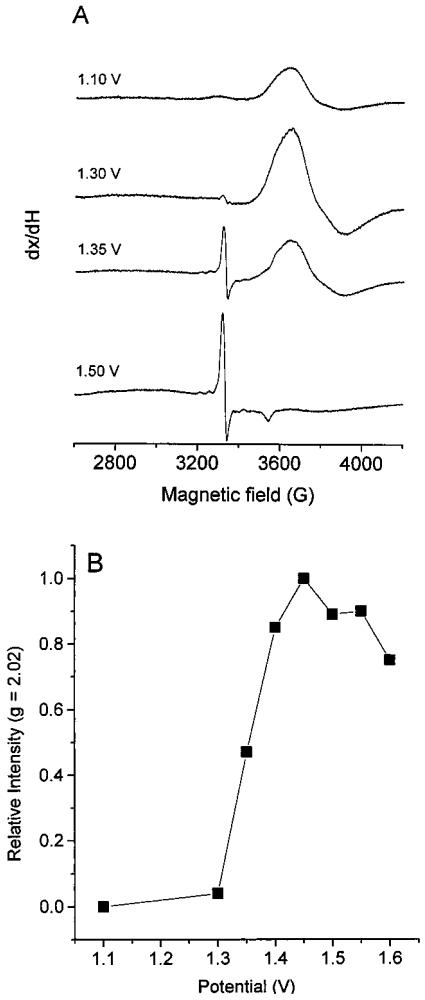

Figure 9. X-band EPR spectra of flow-electrochemically oxidized μ-oxo dimer: (A) 1 mM total complex ion in 0.5 M triflic acid poised at the indicated redox potentials; (B) relative peak heights of the $g = 2.02$ signal at different electrolysis potentials. Conditions: single scans at 9.482 GHz microwave frequency; 2.02 mW microwave power; 15 K; 20 G modulation amplitude; 9.5 G/s scan rate.

of weakly resolved hyperfine interactions. In contrast, the broad axial signal observed at intermediary levels of oxidation appeared only at concentrations above ~1 mM, and may therefore be an associated form of the complex. Furthermore, because this signal disappeared from samples oxidized above ~1.45 V (Figure 9A), it must involve an intermediary oxidation state of the dimer. The intensities of both EPR signals diminished progressively with increasing temperature and were not detectable above ~100 K.

Identity of the Oxygen-Evolving Species. Initial rates of μ-oxo dimer-catalyzed water oxidation by Ce^{4+} in 0.5 M triflic acid at room temperature were found to be linearly dependent upon the total added catalyst concentration over the range of 0.05−0.2 mM. These results are consistent with previous studies using Co^{3+} as the oxidant,[24] and indicate that O_2 is obtained from decomposition of a single catalyst ion. If the [5,5] ion is the oxygen-evolving species, or an immediate precursor to other species that rapidly evolve O_2, then the rate constant for its decay to the [4,4] oxidation state determined in the absence of chemical oxidants should equal twice the steady-state catalytic turnover rate constant (k_{cat}) for O_2 formation. The 2-fold difference follows from the stoichiometry of the net reaction, 2[5,5] → 2[4,4] + O_2. Turnover rate constants were estimated from the dependence of initial rates of O_2 formation upon catalyst concentration under conditions where Ce^{4+} was in (100−400)-fold excess, and consequently oxidation of the dimer to the [5,5] state was nearly quantitative. Values obtained for both the underivatized dimer and the 4,4′-dimethylbipyridine analogue were $k_{cat} = 1.3 \times 10^{-2}$ s^{-1}. Allowing for slightly differing medium conditions and the inherent difficulties in measuring accurately O_2 formation rates,[24] these values are in reasonable agreement with the directly measured rate constants for decomposition of the [5,5] ions to the [4,4] ions, i.e., $k = (9.5-9.9) \times 10^{-3}$ s^{-1}. By this analysis, the [4,4] ion can be excluded as the O_2-evolving species, since its decomposition rate constant (Figure 5B) is much slower than k_{cat}.[25] Alternatives to the [5,5] ion could be other oxidation states formed by its disproportionation, e.g., 2[5,5] ⇌ [4,5] + [5,6], which might rapidly generate O_2 or H_2O_2.[26] However, no evidence was found in the optical or RR flow-spectroelectrochemical experiments for a thermodynamically accessible higher oxidation state, so that the minimal interpretation consistent with the available data is that the [5,5] ion is the O_2-evolving oxidation state.

Comparison to Other Studies. The combined results clearly indicate that the [3,3] ion can be quantitatively oxidized to the [5,5] state, which then undergoes slow decomposition with evolution of O_2; other stable oxidation states in the catalytic cycle include the [3,4] and [4,4] ions. Assignment of the higher oxidation state to the [4,4] ion differs from our earlier assignment as the [4,5] ion,[15] which was based on published electrochemical studies[11] and our assumption that the low-temperature EPR signal observed at intermediary levels of oxidation arose from a monomeric odd-spin system. The concentration dependence of this signal strongly suggests that it arises from a molecular aggregate, and that the monomeric intermediate is EPR-silent, consistent with an even-spin, i.e., [4,4], oxidation state. This assignment also rationalizes a long-standing puzzle concerning the RR spectra, namely, why only the [5,5] ion showed a ruthenyl terminal oxo stretching band in the 800 cm^{-1} region (Figure 3). As the [4,5] ion, the intermediate might also be expected to have a fully deprotonated terminal ruthenyl oxygen, but as the [4,4] ion, these oxo ligands are more likely to be protonated, i.e., exist as coordinated hydroxyl groups, in acidic solutions.

Our conclusions also differ markedly from those of a recent published study[10] of the kinetics of oxidation of the [3,4] ion by Ce^{4+} ion and cross-reactions of dimers prepared in various oxidation states. Using global kinetic analysis to fit temporal changes in the optical spectra, Meyer and associates concluded (i) that the [5,5] ion never accumulates in the catalytic cycle because its decomposition, which is accompanied by O_2 evolution, is relatively rapid and (ii) that the [4,4] ion is unstable with respect to disproportionation to the [3,4] and [4,5] oxidation states. Consequently, they have argued that the O_2-evolving process cannot be directly measured, and the species that accumulate during catalytic turnover in the presence of excess oxidant are the [3,4] and [4,5] ions. However, our redox titrimetric result with $Os(bpy)_3^{2+}$ (Figure 4) clearly shows that the [5,5] ion does accumulate and undergoes slow decomposition

(24) Lei, Y.; Hurst, J. K. *Inorg. Chim. Acta* **1994**, *226*, 179−185.

(25) Decay of the [4,4] ion is complex and may not proceed through intermediary formation of the [5,5] ion when strong chemical oxidants are absent. When excess Ce^{4+} or Co^{3+} is present, however, the catalytic cycle involves oxidation of the [4,4] ion by these ions to the [5,5] state.

(26) Reasonable mechanisms involving disproportionation of [5,5] as the first step can be written which predict first-order decay of the [5,5] ion. For example, the sequence (1) 2[5,5] ⇌ [4,5] + [5,6]; (2) [5,6] → [3,4] + O_2; (3) [3,4] + [4,5] → 2[4,4] is first order when step 2 is rate limiting and the equilibrium position for step 1 lies far to the left.

(Figure 5A) at a rate that corresponds to catalytic turnover. Furthermore, the experiments mixing equal amounts of [3,3] and [5,5] (Figure 6) clearly indicate stoichiometric formation of [4,4], rather than equimolar mixtures of the [3,4] and [4,5] ions. These two studies were made under different medium conditions, i.e., 1 M $HClO_4$ (ref 10) vs 0.5 M triflic acid (this work). While these are seemingly small differences, it has long been known that the [4,4] and [5,5] ions precipitate at these concentrations in media containing 1 M perchlorate ion;[21] indeed, we selected triflic acid to avoid that complication. Meyer and co-workers also noted this precipitate;[10] perchlorate anation or aggregation of the complex, e.g., as discussed below, might account for the apparently disparate results.

Structures of the Highly Oxidized Complex Ions. Anions that are nominally weakly coordinating, such as sulfate,[27] are capable of binding at the aqua positions in the higher oxidation states of *cis*,*cis*-$[L_2Ru(OH_2)]_2O^{n+}$ ions. These aquated complexes display markedly altered redox properties, as exhibited by their cyclic voltammograms.[27] To investigate whether triflate might similarly coordinate the [5,5] ion during its electrochemical synthesis, we compared the CV of an effluent solution from the flow electrolysis cell poised at 1.54 V vs Ag/AgCl with the CV of the unoxidized reagent solution, which contained 0.25 mM [3,3] in 0.5 M triflic acid. The effluent was introduced directly into a small vial containing glassy carbon working, Pt wire counter, and Ag/AgCl reference electrodes poised at an initial potential of 1.5 V. After preconditioning the solution for 5 s, the potential was cycled cathodically to 0.6 V. Two waves were observed, with midpoint potentials at 1.31 and 0.87 V. This CV was nearly identical[28] with that obtained for the [3,3] reagent solution, scanned anodically from 0.6 to 1.5 V, and also appeared indistinguishable from previously published CVs for the [3,3] ion.[11] Scans of effluent solutions were made as soon as 30 s following discharge from the flow cell and, apart from small variations in peak currents, the CVs were unchanged for periods as long as 3600 s following electrolysis. Selected voltammograms are given as Figure S2 in the Supporting Information. We conclude that formation of triflate-bound coordination complexes during electrochemical preparation of the [5,5] ion is negligible.

Although additional work will be required to fully characterize the monomeric [5,5] ion and the low-temperature ion-associated species, it is instructive to briefly consider their unusual EPR and RR spectra. The EPR signal assigned to the [5,5] ion has properties suggestive of formation of a ligand radical, including $g \sim 2.02$ axial symmetry, and partially resolved hyperfine interactions, which could arise from interaction with the ^{99}Ru and ^{101}Ru nuclei ($I = {}^5/_2$, relative abundances 13% and 17%) to give six-line spectra with hyperfine coupling constants of $A \simeq 40$ G (Figure 9). If so, the radical species may bear some functional relationship to oxidation states containing organic radicals that have been detected in the water oxidation cycle of the "dimer-of-dimer" tetranuclear Mn oxygen-evolving complex of photosystem II.[7,29,30]

A decrease in covalency of the terminal oxo ligands of the [5,5] ion upon Ce^{4+} coordination is suggested from the large frequency shift from 818 to 683 cm^{-1} in its RR spectrum (Figure 7). The relatively large shift in the Ru−O−Ru symmetric stretching frequency at 409 cm^{-1} ($\Delta\nu = -20$ cm^{-1}) upon substitution of ^{18}O in the bridge also indicates considerable distortion of the normal dimeric structures. For many single and multiply bridged μ-oxo complexes, the M−O−M bond angle can be accurately estimated[20] from the magnitude of the ^{18}O-induced shift in this band by using the secular equations developed by Wing and Callahan.[19] In the present case, the 20 cm^{-1} shift predicts a Ru−O−Ru bond angle of ∼90°, which can be compared to Ru−O−Ru angles of 160−170° calculated from the corresponding isotopic shifts for the [3,3],[21] [3,4], [4,4], and [5,5] ions in solution. However, the position of the band at 409 cm^{-1} is ∼150 cm^{-1} too low to be assigned to an isolated Ru−O−Ru stretching mode with this bonding angle.[19,20] Thus, it appears from this simple analysis that ion association is accompanied by conformational perturbations that are sufficiently large to mix the Ru−O−Ru stretching frequency with other vibrations. A plausible mode of Ce^{4+} coordination to the [5,5] ion is by chelation of the ruthenyl oxygens to form a six-membered trinuclear ring in which each metal ion is bridged to its neighbors by two μ-oxo atoms.

The concentration dependence noted for the broad $g = 1.8$ EPR signal (Figure 9) suggests that other aggregates may form upon cooling partially oxidized solutions. In this case, the solutions were electrochemically oxidized, precluding any Ce^{4+} involvement. Spatially, the μ-oxo dimers appear as hemispheres with the terminal oxo ligands projecting outward from the center of the flat surface.[11] Cofacial dimerization could lead to a "dimer-of dimers" structure in which each Ru is equivalent and linked to two neighboring Ru atoms by one μ-oxo and one μ-peroxo bridge or, with loss of 1 equiv of O_2, by two μ-oxo bridges. Association through the ruthenyl *cis*-oxo ligands would destabilize the [5,5] oxidation state and favor comproportionation of a ([4,4] + [5,5]) dimer-of-dimers to a $([4,5])_2$ electronic arrangement, which should be EPR detectable.

Di-μ-oxo bridged iron and copper complexes that adopt a diamond bridging geometry show strong RR bands at 600−690 cm^{-1} that have been assigned to the totally symmetric vibration of the $M_2(\mu\text{-}O)_2$ cores.[31,32] The isotopic shifts obtained upon ^{18}O-substitution in the bridging positions ($\Delta\nu = -(20-30)$ cm^{-1}) are also unchanged in D_2O, but are somewhat smaller than those we have measured ($\Delta\nu \approx -(45)$ cm^{-1}, Figure 8). The di-μ-oxo copper complexes have been shown to transform reversibly into a μ-η^2:η^2-O_2 bound species upon changing the solvent composition of the medium.[31] This facile interconversion has been proposed as the mechanism of O_2 evolution in the manganese cluster of photosystem II. This, however, is not the mechanism of O_2 evolution from the Ru μ-oxo dimers studied here because it would predict isotopic substitution of ^{18}O in the Ru−O−Ru bridge after a single turnover, whereas none was observed after ≳10 turnovers.

Acknowledgment. The authors are indebted to several individuals at the Oregon Graduate Institute (Portland, OR), including Professor Thomas Loehr for generously making available his Raman facility for these studies, Dr. Pierre Moënne-Loccoz for expert tutelage and assistance in acquiring the RR data, and Professor Joann Sanders-Loehr for insightful

(27) See, e.g.: Rotzinger, F. P.; Munavalli, S.; Comte, P.; Hurst, J. K.; Gratzel, M.; Pern, F.-J.; Frank, A. J. *J. Am. Chem. Soc.* **1987**, *109*, 6619−6626.

(28) A barely detectable minor component was observed at ∼0.7 V (Figure S2); this feature, which was invariant with time, was not present in the CV of the [3,3] reagent solution.

(29) Boussac, A.; Zimmerman, J.-L.; Rutherford, A. W.; Lavergne, J. *Nature* **1990**, *347*, 303−306.

(30) Ono, T.; Inoue, Y. *FEBS Lett.* **1991**, *278*, 183−186.

(31) Halfen, J. A.; Mahapatra, S.; Wilkinson, E. C.; Kaderli, S.; Young, V. G., Jr.; Que, L., Jr.; Zuberbühler, A. D.; Tolman, W. B. *Science* **1996**, *271*, 1397−1400.

(32) Dong, Y.; Fujii, H.; Hendrich, M. P.; Leising, R. A.; Pan, G.; Randall, C. R.; Wilkinson, E. C.; Zang, Y.; Que, L., Jr.; Fox, B. G.; Kauffman, K.; Münck, E. *J. Am. Chem. Soc.* **1995**, *117*, 2778−2792.

discussions. The authors also thank Dr. Michael Finnegan at Washington State University for assistance in acquiring the EPR data and Mr. James Sylva (WSU) for preparing some of the ruthenium complexes used in the study. This research is supported by the Division of Chemical Sciences, Office of Basic Energy Sciences, U.S. Department of Energy, under Grant DE-FG06-95ER14581.

Supporting Information Available: A figure (S1) illustrating loss of oxidizing equivalents accompanying decay of the [5,5] ion; a figure (S2) giving cyclic voltammograms of the electrochemically prepared [5,5] ion (PDF). This information is available free of charge via the Internet at http://pubs.acs.org.

JA993914Y